

Large oscillating non-local voltage in multi-terminal single wall carbon nanotube devices

G. Gunnarsson, J. Trbovic, and C. Schönenberger

Department of Physics, University of Basel, Klingelbergstrasse 82, CH-4056 Basel, Switzerland

We report on the observation of a non-local voltage in a ballistic (quasi) one-dimensional conductor, realized by a single-wall carbon nanotube with four contacts. The contacts divide the tube into three quantum dots which we control by the back-gate voltage V_g . We measure a large *oscillating* non-local voltage V_{nl} as a function of V_g . Though a classical resistor model can account for a non-local voltage including change of sign, it fails to describe the magnitude properly. The large amplitude of V_{nl} is due to quantum interference effects and can be understood within the scattering-approach of electron transport.

PACS numbers: 73.23.-b, 73.23.Ad, 73.63.Fg, 73.63.Nm, 73.63.Kv, 72.80.Rj

The recent realization of the spin field-effect transistor in carbon nanotube (CNT) devices [1] demonstrated the ability to control spin transport in a quantum dot (QD) [2]. However, additional effects, such as the anomalous magnetoresistance, can contribute to the observed signal in spin-valves [3, 4, 5, 6]. It seems clear, that despite a number of large responses seen in CNT-based devices [1, 7, 8, 9], one needs to go beyond two terminal structures by realizing multi-terminal devices where non-local measurements are feasible [10]. The non-local measurement in spin-valve devices has been pioneered by Johnson and Silsbee [11] in metallic spin-valves and was further applied to various other systems [12, 13, 14]. This technique separates spin from charge effects. Recent application of the *non-local* spin technique in CNTs [10] showed the feasibility and yet tremendous challenge of performing such measurements in low dimensional mesoscopic systems. The hallmark of these measurements is that a positive voltage is measured when the magnetization of the injector and detector electrodes are parallel and a negative *only* when they are antiparallel. However, it has been reported recently that the four-probe resistance with non-magnetic probes in CNTs can be negative due to interference effects [15]. This suggests that the measurement of the *non-local* spin transport in mesoscopic systems like CNTs with ferromagnetic contacts should be strongly influenced by quantum interference effects.

We report here on measurements of a large non-local voltage V_{nl} in multi-terminal CNT devices (Fig. 1a) in the quantum-dot (QD) regime which changes sign and magnitude as the back-gate voltage is swept. We show that V_{nl} cannot be explained by a classical resistor model. Instead, a quantum approach is required. We also show that in these devices, which have relative transparent contacts with resistances in the range of 10 – 100 k Ω , the magnitude of the oscillating V_{nl} greatly exceeds any non-local spin signal.

Our devices consist of single-wall CNTs grown by chemical vapor deposition (CVD) and contacted with four probes as shown in Fig 1a. Two middle electrodes are ferromagnetic (F) made of

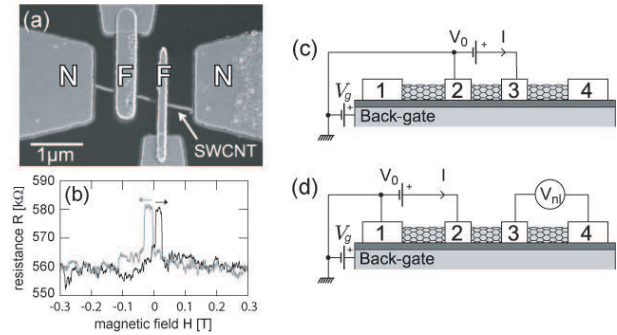


FIG. 1: (a) An SEM-image of a device. The metallic single-wall CNT is contacted with two ferromagnetic (F) and two normal contacts (N), which together divide the tube into three equidistant segments ($L \approx 500$ nm) which act as QDs. (b) Two terminal magneto-resistance signal (F-F). (c,d) Schematics of the measurement setup for the local two-terminal (c) and non-local four-terminal (d) measurement.

PdNi(20nm)/Co(25nm)/Pd(10nm) tri-layer, whereas the two outer probes are normal (N) Pd(40nm) electrodes. A PdNi alloy with 30% Pd is used, because it makes stable contacts to the CNT [1], while Co serves as magnetization alignment layer for PdNi [16]. The device lies on a 400 nm thick SiO_2 layer, with an underlying highly doped Si substrate which is used as a back-gate. The CNT was localized with a scanning-electron microscope (SEM) and the structure was defined using electron-beam lithography.

Samples were cooled in a He4 cryostat to 1.8K where the differential conductance ($G = dI/dV_0$) was measured using standard low frequency lock-in technique with an excitation voltage of $V_0 = 100 \mu V$. Two terminal local G -measurements were made across the three segments of the sample (schematics in Fig 1c) in the gate voltage range $V_g = 1.4 - 2.4$ V, see Fig. 2a-c. G is found in the range of 0.1 to $2 e^2/h$ and strongly varies as a function of V_g , as expected for a QD. By sweeping a DC source-drain voltage V_{sd} we have obtained a gray-scale plot of G for the right segment 3–4 (inset of Fig 2c). The conductances of the three segments display qualitatively similar patterns

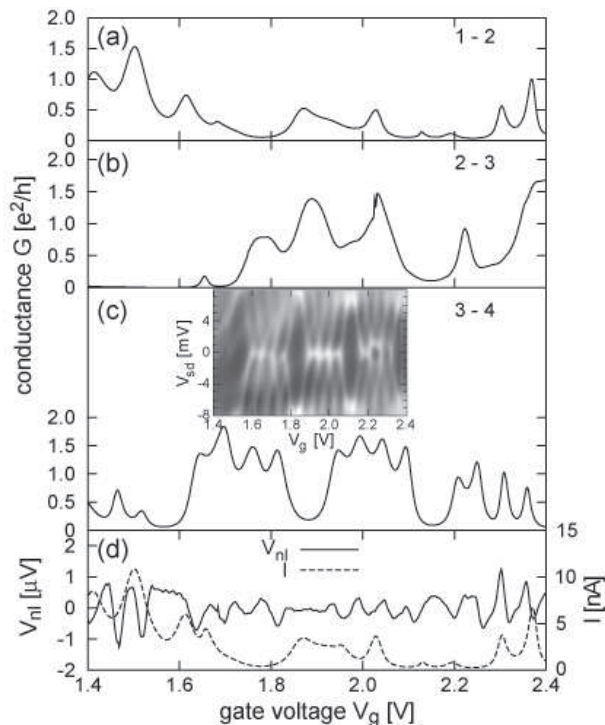


FIG. 2: (a-c) Linear conductance G of each segment of the device as a function of gate voltage V_g . The inset of c shows a gray-scale plot of dI/dV_0 as function of V_g and source-drain bias V_{sd} in the same V_g range. (d) Non-local voltage measured across terminals 3 and 4 (full curve) and the current injected across terminals 1 and 2 (dashed).

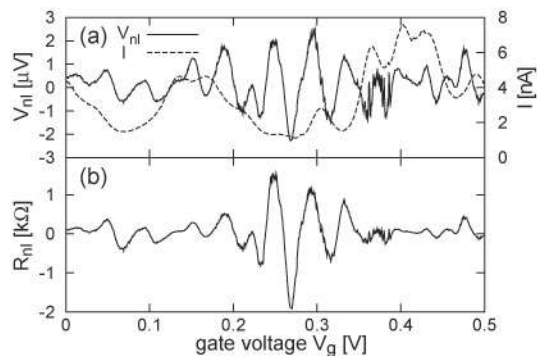


FIG. 3: Non-local measurement as function of gate voltage V_g of another device. (a) The current I between terminals 1-2 (dashed) is plotted together with the non-local voltage V_{nl} between terminals 3-4 (solid). (b) Calculated non-local resistance $R = V_{nl}/I$.

in different V_g -ranges, but the fine structure may vary. This particular V_g -range has been selected for Fig. 2, because of the pronounced four-fold pattern [17, 18] in the detection arm of the non-local measurement, proving the absence of intratube scattering, and the presence of a QD formed by an *individual* single-wall CNT.

The non-local voltage measured across segment 3-4 is shown in Fig 2d (full) together with the current I (dashed curve) injected through segment 1-2 and driven by a constant ac voltage V_0 of $200 \mu V$. Two most striking features are noticeable in these measurements. First, the non-local voltage V_{nl} oscillates around zero, and secondly, the amplitude is large with a typical value of $1 \mu V$. This results in an oscillating non-local resistance $R_{nl} = V_{nl}/I$ with values of $0.1 - 1 k\Omega$. A similar behavior is found in different gate-voltage ranges, as well as in different samples, see e.g. Fig. 3.

In order to understand the origin of the observed signal, we first model our device as a classical network of resistors, shown in Fig. 4a [10]. Each terminal in the circuit is characterized by contact resistances R_{ci} and r_{ci} and the CNT sections between terminals i and its next neighbors j have resistances R_{ij} . Two limiting cases are shown in (b) and (c) of Fig. 4: in case (b) of ‘non-invasive’ contacts ($R_c \gg r_c$), all contacts 1-4 couple weakly to the CNT. In contrast, in case (c) of ‘strongly invasive’ contacts ($R_c \ll r_c$), the CNT is split into segments. Although there have been reports on both strong and weak contacts to CNTs [19], a typical device lies in between. For weak contacts (Fig. 4b), driving a current in the left branch results in the appearance of a *uniform* voltage V' on the CNT. Hence, $V_3 = V_4 = V'$ and the non-local voltage $V_{nl} := V_3 - V_4 = 0$. For strong contacts (Fig. 4c), V_3 and V_4 equal the bias voltage V_0 , leading again to a vanishing non-local voltage. Because we have assumed ideal voltage probes in which no current flows, the right arm must have a uniform potential also in the general case. We therefore conclude that $V_{nl} = 0$ in the classical limit. This breaks down, if the electrometers are not ideal, but possess a finite input impedance, thereby providing a current sink.

We next take the input amplifier input impedances $R_I = 100 M\Omega$, appearing at the voltage probes 3 and 4, in the resistor model in Fig. 4a into account. Assuming a ballistic wire with $R_{ij} = 0$, we obtain for V_{nl} of the third segment (3-4): $V_{nl} \approx V_2^*(r_{c3} + r_{c4} + R_{c4} - R_{c3})/R_I$, where V_2^* is the potential at the inner node of contact 2, as shown in Fig. 4a. V_2^* is of order V_0 . Note, that because of the minus sign in one term, a negative V_{nl} is possible for certain resistance values. If the magnitude of all contact resistances were similar, however, a positive ‘mean’ non-local voltage is predicted in disagreement with the experiment. The observation of an oscillating V_{nl} with a mean value close to zero could only be reconciled with the classical model if $r_c \ll R_c$. Then, the equation simplifies and we arrive at the following estimate: $V_{nl} \approx V_0(R_{c4} - R_{c3})/R_I$. This formula predicts that V_{nl} follows the gate-voltage behavior of the resistances of contact 3 and 4. Using a typical contact resistance for our device of $100 k\Omega$, $R_I = 100 M\Omega$, and $V_0 = 200 \mu V$, we estimate $V_{nl} \sim 0.2 \mu V$. This is an order of magnitude smaller than measured in the experiment, where the oscillating non-local voltage peaks up to $V_{nl} \sim 2 \mu V$. In order to be absolute certain that

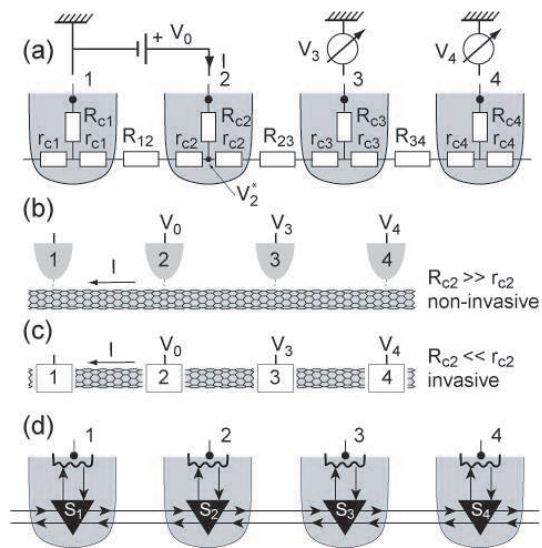


FIG. 4: (a) Resistor model for metal-CNT contacts. The three resistors in each shaded region model the property of the contact, whereas R_{34} , for example, describes the intra-tube resistance in between contact 3 and 4. Two limiting cases are shown in (b) and (c): In (b) the contacts are weakly coupled to the CNT, whereas they split the CNT into segments due to their strong coupling in (c). (d) shows the quantum description, using three-port scattering matrices S_j (triangles) in each node. Note, that there is an additional input resistance R_I (not shown) in both electrometers measuring V_3 and V_4 .

the current in the detector arm caused by the finite impedance R_I of the amplifiers is not the source of V_{nl} , we have crossed-checked these measurement with a custom-modified amplifier with an input impedance of $R_I = 1 \text{ G}\Omega$ and have found no change in V_{nl} . We are therefore confident that the classical resistor model cannot account for the measured oscillating non-local voltage V_{nl} and that the finite input impedance of the amplifiers is not the source of this signal.

To understand the magnitude of the non-local voltage, we next move on to a quantum-coherent description. We apply the scattering approach [20] to calculate V_{nl} . A similar approach has been taken by Lerescu *et al.*, but for an open cavity that supports many modes [21]. In contrast, in our case of a CNT we deal with a (quasi) one-dimensional (1d) system. This approach is sketched in Fig. 4d. The triangles in each node j denote a three-port scattering matrix S_j . If we assume that each port is described by a one mode conductor, S_j is a 6×6 matrix that describes the amplitudes between outgoing and incoming waves [20]. If we stick to a one-mode conductor, one can prove that $V_{nl} = 0$, independent of any details of S_j . This theorem of vanishing non-local voltage in a 1d conductor can be traced back to the particular structure of the whole S matrix in which the S_j 's are connected *in series*. Hence, similar to the resistor model, even in the coherent description, the non-local voltage is expected to disappear, provided the wire is 1d. Be-

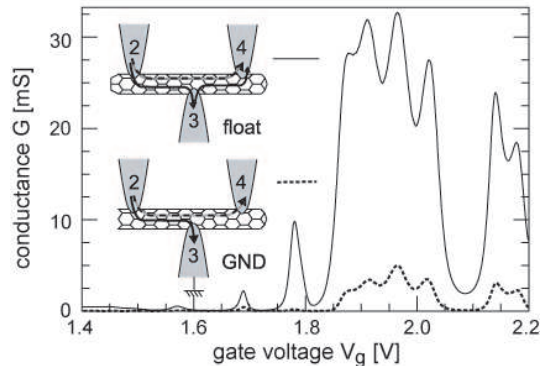


FIG. 5: Measurements of the two-terminal conductance G_{42} between terminals 2 and 4 while terminal 3 is floating (line) and while it is grounded (dashed line). The inset depicts transmission through the CNT in both cases.

cause we do measure a large V_{nl} in our devices, one of the assumption in the theorem must be violated. These are: linear response and truly 1d. To the former, we note that the maximum applied voltage of $200 \mu\text{V}$ corresponds to 2.3 K which is slightly above the measurement temperature. But we have also measured at $100 \mu\text{V}$ and below confirming linearity. To the latter we emphasize that V_{nl} does not change with the relative magnetization direction of the two ferromagnetic contacts, so that the spin degeneracy is not lifted. What remains as an explanation is the fact that due to the so-called K and K' degeneracy of graphene [22] any CNT should carry two (orbitally) degenerate 1d modes. This then leads to the well-known four-fold pattern [17, 18] in the spectrum of a CNT-QD, which is clearly visible in Fig. 2c.

In order to estimate V_{nl} , we use the Landauer-Büttiker formalism [20]. The current I_i in lead i is given by $I_i \propto (N - R_i)V_i - \sum T_{ij}V_j$, where N denotes the number of modes (here $N = 2$), R_i the total reflection coefficient for contact i , T_{ij} the probability that a charge carrier is transmitted from contact j to contact i , and V_k the potential at contact k . Using this formalism, one can derive a compact formula for a general four terminal voltage [20]. For our geometry one obtains $V_{nl} = V_0(T_{32}T_{41} - T_{42}T_{31})/D$, where the denominator D is given by: $D = (N - R_4)(N - R_3) - T_{34}T_{43}$. This expression can only be evaluated (estimated) if we can, in addition to nearest neighbor transmissions, estimate the transmission probabilities that embrace second or even third-nearest neighbor contacts. These are the coefficients T_{31} , T_{42} , and T_{41} . For the former two, the electron wave has to be able to transmit *under* one contact (2 or 3) without relaxation, while for the latter even both contacts 2 and 3 need to be passed. We estimate this transmission beneath a contact by comparing the conductance G_{42} between terminals 2 and 4 when contact

3 is floating or grounded. The result is shown in Fig. 5. If the intermediate contact is floating, electrons that are transmitted into contact 3 must be re-injected into the device so that the transmission between 2 and 4 can be large. On the other hand, for rather strong-coupling contacts as ours, only a small fraction of electrons is expected to transmit unperturbed under the contact. If contact 3 is now grounded, most carriers disappear via contact 3 to ground. This latter situation is indeed realized as shown in the data of Fig. 5. The dashed curve is suppressed by approximately a factor of 7 – 8. Hence, a fraction of 13% can pass under the contact by direct transmission [23]. This is surprisingly large taken the typical values of the two-terminal resistances and the fact that the metal electrodes were evaporated directly onto a freshly CVD-grown CNT. Let us assume that transmission under the contact is similar for contact 2 and 3 and let us denote this probability by t . The magnitude of V_{nl}/V_0 is then estimated by t^2 , so that $|V_{nl}| \lesssim 3.5 \mu\text{V}$, in good agreement with the measured V_{nl} .

We now turn our attention to spin transport and estimate the expected spin-dependent non-local voltage V_{nl}^{spin} . We use the resistor model shown in Fig. 4. This time, however, one has to expand it by introducing separate spin up and spin down channels. The contact resistances at F contacts depends on the relative orientation of the electron spin and the magnetization within the F contacts [10]. For simplicity we assume that different contacts have equal resistances. We emphasize here, that for the detection of a non-local spin signal, the spin-imbalance in the injector part 1-2 has to be able

to ‘diffuse’ into the detector branch. In the strongly invasive limit this is impossible, because the strongly coupled contact 2 would equilibrate the spin-imbalance. In contrast, for weakly coupling contacts, a spin imbalance in the CNT caused by spin injection can be sensed by a F contact. V_{nl}^{spin} therefore strongly depends on the ratio $r := r_c/R_c$. Assuming a small contact polarization p , one obtains $V_{nl}^{spin}/V_0 = p^2 \cdot 0.25$, if $r \ll 1$, which is the largest possible signal. Using the measurement shown in Fig. 5, we can estimate the r -ratio for our devices. We obtain $r \simeq 6$. This then yields $V_{nl}^{spin}/V_0 \simeq p^2 \cdot 0.0037$. We estimate p from the typical two-terminal TMR of $\approx 4\%$ [1], yielding a polarization of $\approx 20\%$. Inserting p and $V_0 = 200 \mu\text{V}$, the expected spin-dependent non-local voltage is only $V_{nl}^{spin} \simeq 30 \text{ nV}$, two-orders of magnitude smaller than the measured non-local voltage.

In conclusion, we find large oscillating non-local signals in all of our CNT quantum-dot devices. The existence of such a background, which changes its sign with the back-gate voltage can screen the non-local signals due to spin in particular in devices with relative high contact transparency.

Note: After completing this work, we have become aware of a similar, but independent study by A. Makarovski *et al.* [23].

Acknowledgement: Support by the Swiss NSF, the NCCR on Nanoscale Science, and EU-FP6-IST project HYSWITCH is gratefully acknowledged. Fruitful discussions with B. J. van Wees are gratefully acknowledged.

-
- [1] S. Sahoo, T. Kontos, J. Furer, C. Hoffmann, M. Gräber, A. Cottet, and C. Schönberger, *Nature Phys.* **1**, 99 (2005).
- [2] S. J. Tans, M. H. Devoret, H. Dai, A. Thess, R. E. Smalley, L. J. Georliga, and C. Dekker, *Nature* **386**, 474 (1997); M. Bockrath, D. H. Cobden, P. L. McEuen, N. G. Chopra, A. Zettl, A. Thess, and R. E. Smalley, *Science* **275**, 1922 (1997); D. H. Cobden, M. Bockrath, P. L. McEuen, A. G. Rinzler, and R. E. Smalley, *Phys. Rev. Lett.* **81**, 681 (1998).
- [3] see for example: H. X. Tang, F.G. Monzon, M. L. Roukes, F.J. Jedema, A.T. Filip and B.J. van Wees in *Semiconductor Spintronics and Quantum Computation*, D. D. Awschalom, N. Samarth and D. Loss eds., Springer Verlag (Berlin 2002).
- [4] H. X. Tang, R. K. Kawakami, D. D. Awschalom, and M. L. Roukes, *Phys. Rev. Lett.* **90**, 107201 (2003).
- [5] C. Gould, C. Rüster, T. Jungwirth, E. Girgis, G. M. Schott, R. Giraud, K. Brunner, G. Schmidt, and L.W. Molenkamp, *Phys. Rev. Lett.* **93**, 117203 (2004).
- [6] S. J. van der Molen, N. Tombros, and B. J. van Wees, *Phys. Rev. B* **73**, 220406 (2006).
- [7] H. T. Man, I. J. W. Wever, A. F. Morpurgo, *Phys. Rev. B* **73**, 241401 (2006).
- [8] B. Zhao, I. Mönch, H. Vinzelberg, T. Mühl, and C. M. Schneider, *Appl. Phys. Lett.* **80**, 3144 (2002).
- [9] L. E. Hueso, J. M. Pruneda, V. Ferrari, G. Burnell, J. P. Valdes-Herrera, B. D. Simons, P. B. Littlewood, E. Artacho, A. Fert, and N. D. Mathur, *Nature* **445**, 410 (2007).
- [10] N. Tombros, S. J. van der Molen, and B. J. van Wees, *Phys. Rev. B* **73**, 233403 (2006).
- [11] M. Johnson and R. H. Silsbee, *Phys. Rev. Lett.* **55**, 1790 (1985).
- [12] F. J. Jedema, A. T. Filip, B. J. van Wees, *Nature* **410**, 345 (2001).
- [13] X. Lou, C. Adelman, S. A. Crooker, E. S. Garlid, J. Zhang, K. S. M. Reddy, S. D. Flexner, C. J. Palmstrom, and P. A. Crowell, *Nature Phys.* **3**, 197 (2007).
- [14] N. Tombros, C. Jozsa, M. Popinciuc, H. T. Jonkman, B. J. van Wees, *Nature* **448**, 571 (2007).
- [15] B. Gao, Y. F. Chen, M. S. Fuhrer, D. C. Glatli, and A. Bachtold, *Phys. Rev. Lett.* **95**, 196802 (2005).
- [16] Detailed measurements of the magnetic properties of PdNi/Co bi-layer will be published elsewhere.
- [17] W. Liang, M. Bockrath, and H. Park, *Phys. Rev. Lett.* **88**, 126801 (2002).
- [18] M. R. Buitelaar, A. Bachtold, T. Nussbaumer, M. Iqbal, and C. Schönberger, *Phys. Rev. Lett.* **88**, 156801 (2002).
- [19] see for example: M. Bockrath, D. H. Cobden, L. Jia, A. G. Rinzler, R. E. Smalley, L. Balents, P. L. McEuen,

- Nature **397**, 598 (1999); A. Bachtold, M. de Jonge, K. Grove-Rasmussen, P. L. McEuen, M. Buitelaar, and C. Schönberger, Phys. Rev. Lett. **87**, 166801 (2001).
- [20] M. Büttiker, Phys. Rev. Lett. **57**, 1761 (1986).
- [21] A. I. Lerescu, E. J. Koop, C. H. van der Wal, B. J. van Wees, and J. H. Bardarson, arXiv:0705.3179v1.
- [22] M. S. Dresselhaus, G. Dresselhaus, P. C. Eklund: *Science of Fullerenes and Carbon Nanotubes* (Academic Press, New York 1996).
- [23] A. Makarovski, A. Zhukov, J. Liu, and G. Finkelstein, arXiv:0709.2498v1.
- [24] M. Jullière, Phys. Lett. **54A**, 225 (1975).
- [25] I. Zutic, J. Fabian, and S. Das Sarma, Rev. Mod. Phys. **76**, 323 (2004).